Journal Microsystem Technologies, Volume 15, Number 12, December 2009, Pages 1861-1872

An evaluation of process-parameter and part-geometry effects on the quality of filling in micro-injection moulding

U M Attia*[1] and J R Alcock[2]

*[1] *Building 56, Cranfield University, Wharley End, Cranfield, Bedfordshire, MK43 0AL, UK.* E-mail: u.attia@cranfield.ac.uk. *Tel: +44 (0)1234 750111 ext: 2408*

[2] *Building 61, Cranfield University, Wharley End, Cranfield, Bedfordshire, MK43 0AL, UK*

This paper addresses the use of micro-injection moulding for the fabrication of polymeric parts with microfeatures. Five separate parts with different micro-feature designs are moulded of Polymethylmethacrylate. The design-of-experiments approach is applied to correlate the quality of the parts to the processing parameters. Five processing parameters are investigated using a screening half-factorial experimentation plan to determine their possible effect on the filling quality of the moulded parts. The part mass is used as an output parameter to reflect the filling of the parts. The experiments showed that the holding pressure is the most significant processing parameter for all the different shapes. In addition, the experiments showed that the geometry of the parts plays a role in determining the significant processing parameters. For a more complex part, injection speed and mould temperature became statistically significant. A desirability function approach was successfully used to improve the filling quality of each part.

Keywords: micro-injection moulding, design-of-experiments, geometry, processing parameters, quality control.

1. Introduction

Micro-injection moulding (μIM) is a polymer replication process of high potential for the mass-production of polymeric parts with microfeatures. Mass-production capabilities, high replication fidelity and the ability to process polymers of a wide range of properties are some of the advantages associated with μIM.

For some time the main approach to identify influential processing parameters in μIM was by changing one parameter at a time while keeping the others constant and then observing the effect of this parameter (Wimberger-Friedl 2000; Yao and Kim 2002; De Mello 2002). This approach was inherited from conventional injection moulding, as it was useful in drawing basic conclusions about how each parameter affects the filling quality of the moulded part.

This approach, however, has two main limitations (Eriksson et al. 2008): the first limitation is that it is relatively time consuming when many parameters are being investigated. The second drawback is that it does not take into consideration the effect of the interaction between two or more parameters, which is a relevant consideration in complex processes such as micromoulding.

The design-of-experiments (DOE) approach was introduced into this research domain as a useful alternative to this conventional method. A number of research groups have used a variety of DOE experimentation plans to investigate the relation between processing parameters and part-

filling quality. A summary of the main DOE experiments is available in the literature (Attia et al., 2009).

The responses chosen for the experiments have included, filling quality of micro-sized channels (Mönkkönen et al., 2002), part dimensions (Zhao et al. 2003a; Aufiero 2005; Sha et al. 2007b; Pirskanen et al. 2005; Sha et al. 2007a), flow length (Griffiths et al. 2007; Jung et al. 2007), weld-line formation (Tosello et al. 2007), demoulding forces (Griffiths et al. 2008) and filled volume fraction (Lee et al. 2008). This is a reflection of the main research challenge in micro-moulding, which is the filling of small cavities. The choice of response is informed by such considerations as: is a specific dimension (or dimensions) critical for the part functionality, e.g. the depth of a channel or the diameter of a hole?, or is the order of magnitude of the part mass suitable for measurement?, e.g. variations in the part mass may be too small to be separated from experimental noise. DOE has also been used to minimise injection time, pressure and temperature distribution using a three-dimensional simulation package (Shen et al. 2002).

Results presented in the literature show that different DOE designs yield different outputs. For example, there is disagreement about the importance of holding pressure and injection speed. Furthermore, certain experiments have highlighted interactions between processing parameters which have not been seen in other work. These differences in experimental results may be due to the different geometrical shapes, polymers and experimental set-ups used in each experiment. It would, therefore, seem reasonable to claim that, at present, significant processing parameters in μIM are indentified on case-by-case basis and cannot be generalized for all situations.

This paper addresses the effect of processing parameters on the filling quality of μIM through a design-of-experiments (DOE) approach. In order to focus on the issue of general applicability highlighted above, the most influential processing parameters of five differently micro-structured parts were each investigated. The parts were of high enough mass to allow part mass to be used as the response. The polymer type (Polymethylmethacrylate (PMMA)) and grade were kept constant over the five micro-parts. Optimized processing conditions were calculated and tested for each of the five parts. They were then compared, so that the effect of the part geometry on the filling behaviour of the polymer could be discussed.

It is worth noting in more detail the prior work which is closest to that of this present study. Whilst some DoE-based experimental data are available, in which part geometries have been deliberately varied within a single moulding (Sha et al. 2007b), no prior work exists which assesses geometrically-different whole micro-moulded parts produced using a particular polymer. In the literature (Zhao et al. 2003a; Zhao et al. 2003b), part mass was used as the response for two different micro-parts, but the moulding polymer was also varied: a polyoxymethylene (POM) micro-gear and a polycarbonate (PC) lens array. The micro-gear consisted of a gear-and-shaft arrangement, where the gear diameter was 2.5 mm and the shaft length was 5 mm. It was produced with a three-plate mould with a gate diameter of 0.6 mm. The lens component had overall dimensions of 12 x 3 x 2 mm carrying lens surfaces of radii 0.35 and 0.5 mm with a gate diameter of 0.3 mm. Five processing parameters were evaluated, namely mould temperature, melt temperature, injection speed, metering size, hold pressure time and cooling time. For the gear structure, the holding pressure time and metering size were highlighted as significant parameters. For the lens array, metering size, injection speed and mould temperature were identified as most significant parameters.

2. Experiment

2.1. Methodology and equipment

In this experiment, five parts (*a* to *e*) with micro-scaled features were investigated. The parts, which were components of a microfluidic device, were designed to have the same external dimensions but different sets of features, both on the surface of, and through the component. Different definitions of micromoulding are in the literature (Attia et al. 2009), so the scope of micromoulding in this experiment was "macro" components with micro-structured regions.

The polymer chosen for this study was Polymethylmethacrylate (PMMA) (VS-UVT, Altuglas®). The grade was selected for its ease of flow (MFI = 24 g/10 min) and its optical transparency (light transmittance 92%). The micro-injection moulding machine was a Battenfeld Microsystems 50.

Five processing parameters were investigated as input factors: polymer-melt temperature (T_p), mould temperature (T_m), injection speed (V_i), holding pressure (P_h) and cooling time (t_c). The response (quality parameter) in all experiments was the part mass (W).

The experimental programme was conducted in three stages following the protocol laid out in Eriksson et al.: familiarization, screening, and optimization (Eriksson et al., 2008). These are detailed in Section 2.4. Weighing of the moulded parts was done using a sensitive scale with a readability of 0.01 mg. Experimental data were processed and analysed using Minitab® 15 (Minitab Inc. 2009).

2.2. Part Geometry

The five moulded parts used in this study were all disc-shaped with a diameter of 10 mm and a thickness of 1 mm. The parts were designed to be building elements in a microfluidic device for a medical application. Each of the five components has a different set of micro-features, the majority of which are in place in order to form through-hole features in the final device. Figure 1 presents a schematic half-cross-section diagram of the five part designs (denoted by letters from *a* to *e*) with some of their critical dimensions:

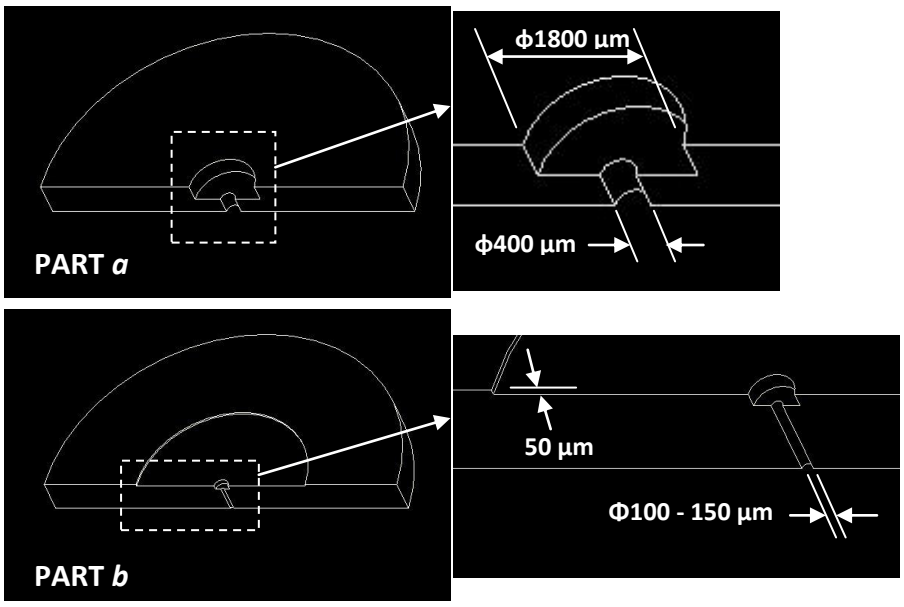

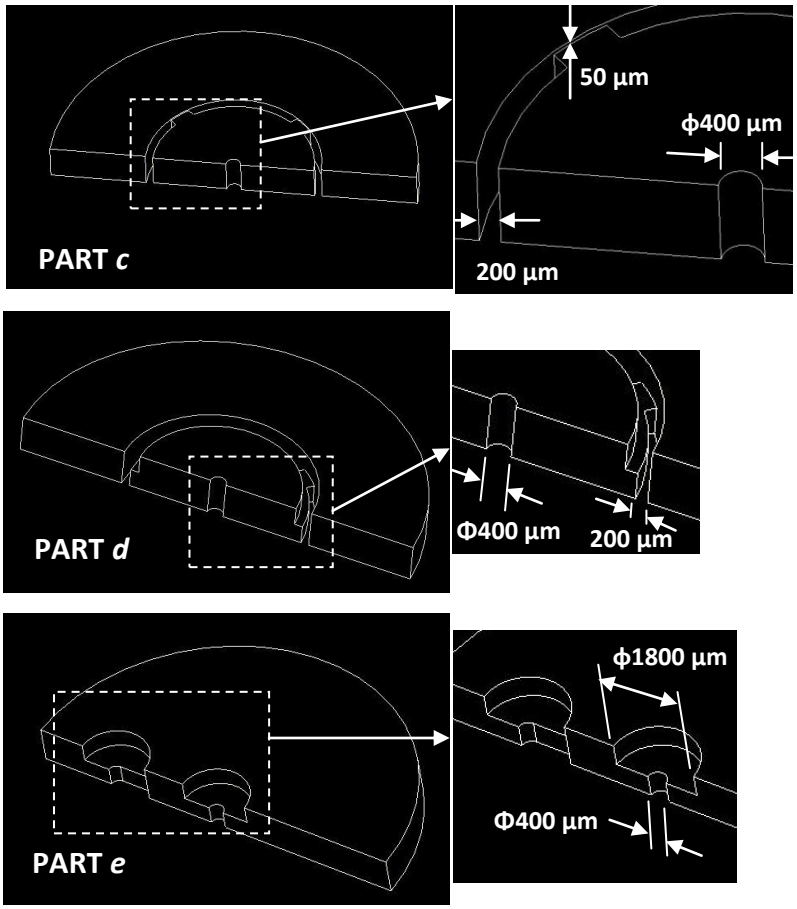

Fig 1 Half-cross-section diagrams of the five parts *a* to *e* with some of the main dimensions highlighted

2.3. Mould manufacturing

Each part was moulded by an individual aluminium mould that was housed within a main steel micro-mould body. A detailed description of the mould design and machining process for the mould inserts can be found elsewhere (Marson et al. 2009). Figure 2 shows SEM images of two of the mould-inserts.

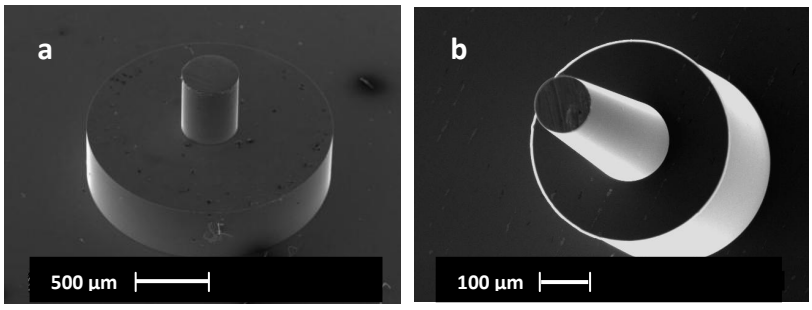

Fig 2 SEM micrographs of the micro-features of mould inserts

2.4. Experimentation stages

2.4.1. Familiarization stage

In the familiarization stage, a set of experiments were conducted in which the selected input parameters were assessed in order to determine the most extreme levels at which the experiment successfully yielded a response. This process window of parameters was then translated to become the high and low levels of the input parameters used in the screening experiments. The metering volumes of the parts were determined experimentally. The volume of each part was selected such that the polymer amount is enough to fill the cavity space without applying any holding pressure. The metering volumes are then kept constant throughout the experiments.

The sampling range was also determined, i.e. the number of moulding cycles after which the process is considered to become stable. Stability was defined as having been achieved when each of the moulded parts possess the same mass within a given tolerance.

The sampling range of the moulding process was determined using statistical control charts. The average mass of the produced parts become stable within the upper and lower limits of the chart after 30 to 40 continuous cycles depending on the mould insert used. As a standard practice, for each set of experimental conditions, samples were randomly collected after 50 cycles.

Table 1 shows the criteria used for selecting the upper and lower values for each parameter.

Factor	Selection criteria	
	Lower level	Higher level
T_p [°C]	The minimum value for this level was the recommendation of the material supplier (around 200°C). Based on experimentation, relatively higher temperatures were selected, such that the injection process ran continuously.	This was selected by experimentation as a safe high limit, above which signs of degradation appeared.
T_m [°C]	The minimum temperature was selected as the temperature recommended by the material supplier.	The high level was selected close to, but below, the Tg of the polymer (approx. 86°C).
P_h [bar]	The minimum holding pressure value was obtained from the literature (Osswald 2001).	The higher holding pressure value was selected not to cause the material to flash.
V_i [mm/s]	This value was selected based on experimentation.	This value was selected based on experimentation.
t_c [s]	The minimum value was calculated as the no-flow time, which is the time by which the gate was actually frozen.	The maximum was selected as approximately twice the minimum.

Table 1. Criteria for selecting the upper and lower levels of the experiment.

Table 2 shows the upper and lower parameter levels selected for each of the five parts in addition to the metering volume selected for each part (including the runner system):

Part	Metering Volume [mm^3]	T_p [°C]		T_m [°C]		V_i [mm/s]		P_h [bar]		t_c [s]	
		Low level (-)	High level (+)	Low level (-)	High level (+)	Low level (-)	High level (+)	Low level (-)	High level (+)	Low level (-)	High level (+)
a	179	240	255	70	81	200	300	250	500	4	7
b	178	230	250	72	80	200	300	100	300	4	7
c	177	230	250	72	84	200	300	100	300	3	6
d	177	230	250	72	84	200	300	100	300	3	6
e	177	230	250	70	84	150	300	100	300	3	6

Table 2. Higher and lower levels for the five tested parameters for the five parts.

2.4.2. Screening stage

The screening stage consisted of the execution of the set of designed experiments. The number of samples and the levels of the input variables were obtained from the familiarization stage. Statistical software and regression models were used to analyse the data. Significant processing parameters and interactions were determined.

The data obtained from the familiarization stage were used in the selected experimentation design. The DOE scheme used was a two-level, half-factorial 16-run (2^{5-1}) design.

This design was selected because it is a resolution-V design, which offers two advantages. Firstly, the number of experimental runs required is half that of a full factorial design. Secondly, this reduction in runs does not affect the results significantly. This is because the main effects are not confounded with other main effects or with second-order interactions and the second-order interactions are not confounded with each other.

The levels of the experimental runs are tabulated in table 3. For each set of experiments, the order in which the experimental runs were conducted was randomized using a built-in randomization function in Minitab.

Standard Order	T_p [°C]	T_m [°C]	P_h [bar]	V_i [mm/s]	t_c [s]
1	-	-	-	-	+
2	+	-	-	-	-
3	-	+	-	-	-
4	+	+	-	-	+
5	-	-	+	-	-
6	+	-	+	-	+
7	-	+	+	-	+
8	+	+	+	-	-
9	-	-	-	+	-
10	+	-	-	+	+
11	-	+	-	+	+
12	+	+	-	+	-
13	-	-	+	+	+
14	+	-	+	+	-
15	-	+	+	+	-
16	+	+	+	+	+

Table 3. A half-factorial, two level 16-run (2^{5-1}) experimentation design.

After stabilisation, ten samples were randomly collected for each run. The average mass of the samples was recorded as the experiment response. The experimental data collected was processed with Minitab® 15 and main-effects plots and Pareto charts were plotted.

One technique for correlating the factors to the response is by regression models. Similar to conventional regression models used to correlate two variables, a regression model can be used to fit the obtained responses to the input factors. The model can be linear, interaction, quadratic or even cubic, depending on the number of experiments conducted (Eriksson et al. 2008). In this particular screening design, an interaction model was selected since it takes into consideration the effect of possible interactions on the response value. The selected regression model takes the following format:

$$y = c + \beta_1 x_1 + \beta_2 x_2 + \beta_3 x_3 + \beta_4 x_4 + \beta_5 x_5 + \beta_{12} x_1 x_2 + \beta_{13} x_1 x_3 + \beta_{14} x_1 x_4 + \ldots \quad (1)$$

In equation (1): y is the response, c is a constant, β values are the model-term coefficients and x_1 to x_5 are factors. The values and signs of the regression coefficients, β, represent the magnitude and the relation of each model term, respectively. Once the coefficients of equation (1) are determined, the response y of any set of given factors can be calculated.

The accuracy of the fit was evaluated by comparing the values of responses calculated from the model, based on the obtained coefficients, to the corresponding actual experimental values.

2.4.3. Determining optimum processing conditions

One approach to optimize the data obtained from the screening stage is to run another round of full factorial designs involving the influential parameters obtained during the screening stage. This approach is usually used when there are a number of influential factors with relatively close effects. A full factorial design would be implemented in this case to optimize the factors with a design that has no confounding factors. In this set of experiments, however, only one or two significant parameters are already identified from the screening stage, so optimization will basically focus on obtaining a suggested set of processing parameters that gives a required value of the response within specified limits.

Optimization was carried out using the desirability function approach to calculate optimum values of the input parameters (Lahey and Launsby 1998; Montgomery 2005). This approach searches for a combination of values for input factors to satisfy a requirement for an output response (or multiple responses). The pre-set requirement of the function would be either to hit a target value within an upper and lower limit, to minimize the response value or to maximize the response value. Another pre-set value of the function is the weight *r*, which specifies the function shape and emphasises (or deemphasises) the target value relative to the limit values.

In case of one response being optimized, the individual desirability can be represented by the equation (Minitab Inc. 2009):

$$d_i = f_i(y)^{Wi} \qquad (2)$$

where *Wi* is the weight of the response, in this case equal to 1, and the function *fi(y)* depends on whether the purpose of the optimisation is to hit a target, minimize or maximize. In this case, the function is desired to hit a target value *T* within upper and lower limits, so it can be represented by the following equation, where *U* and *L* are the upper and lower limits, respectively (Montgomery 2005):

$$f_i(y) = \begin{cases} 0 & y \prec L \\ \left(\dfrac{y-L}{T-L}\right) & L \le y \le T \\ \left(\dfrac{U-y}{U-T}\right) & T \le y \le U \\ 0 & y \succ U \end{cases} \qquad (3)$$

The function in equation (3) is linear because the weight *r* is set to 1. Otherwise, the bracket terms would have been raised to the power r_1 and r_2 that define the weights of the lower and upper limits, respectively.

For each of the five parts investigated in this set of experiments, the target, upper and lower values were selected based on the filling quality of the produced samples. This was undertaken as follows. For each part, after each set of experiments, samples of the 16 runs were inspected under the microscope to check their filling quality. Although each run had a different average mass, one or more runs (i.e. one or more combinations of factors) could have produced completely-filled samples. All the completely filled samples were weighed and an average mass was calculated. The filled samples that had the smallest and the largest masses were also

identified. The average mass calculated from all of the filled samples was set as the target weight for the desirability function. The masses of the filled samples with smallest and largest mass values were used as the pre-set lower and upper limits of the desirability function, respectively.

3. Results

3.1. Responses from the screening experiments

Table 4 shows the average masses in milligrams of the 10 samples collected for each of the five parts:

Standard Order	T_p	T_m	P_h	V_i	t_c	Mass [mg] averaged from 10 samples				
						a	***b***	***c***	***d***	***e***
1	-	-	-	-	+	91.0	86.4	84.8	88.3	86.9
2	+	-	-	-	-	91.2	87.3	85.2	88.5	88.0
3	-	+	-	-	-	91.9	87.8	84.9	88.6	87.5
4	+	+	-	-	+	91.2	87.4	85.3	88.8	89.6
5	-	-	+	-	-	92.5	88.4	87.0	90.0	91.6
6	+	-	+	-	+	93.4	87.9	86.7	89.8	91.6
7	-	+	+	-	+	93.6	88.3	87.2	89.9	91.6
8	+	+	+	-	-	93.8	88.7	87.2	90.5	92.1
9	-	-	-	+	-	90.6	86.6	84.8	87.4	89.3
10	+	-	-	+	+	90.4	86.7	85.0	87.7	88.1
11	-	+	-	+	+	90.7	86.5	85.2	87.8	88.1
12	+	+	-	+	-	91.3	87.3	85.8	88.4	90.7
13	-	-	+	+	+	92.8	88.2	86.5	89.4	90.6
14	+	-	+	+	-	93.2	88.2	87.1	89.6	92.2
15	-	+	+	+	-	93.2	88.0	87.1	89.8	91.0
16	+	+	+	+	+	93.0	88.3	87.3	89.8	92.5

Table 4. Average masses in mg for each of the five parts.

Figure 3 shows a number of SEM micrographs of the replicated plastic parts.

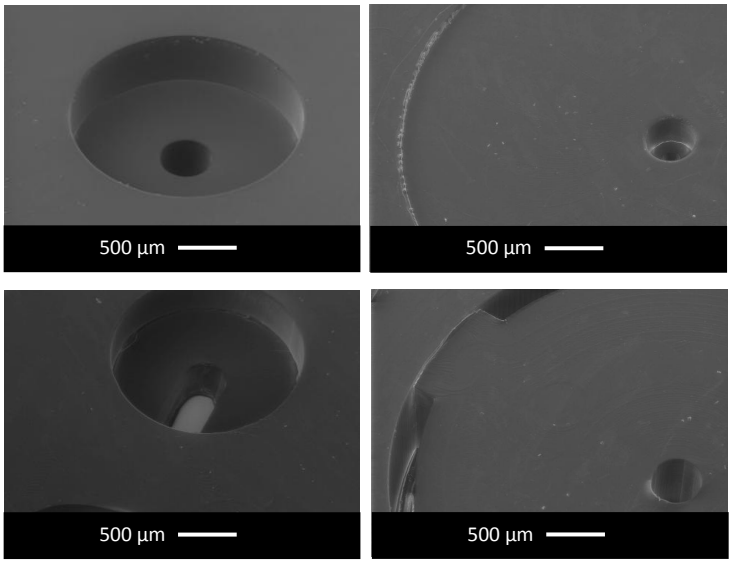

Fig 3 SEM images of some of the replicated plastic parts

Figures 4 to 8 show the Main-effects plots and Pareto charts of standardized effects plotted for the five moulded parts. A main-effect plot for a particular factor is a plot of the average of the data points at the low factor setting and the average of the data points at the high factor setting. The larger the slope of the line that connects the two averages, the more important the

effect is. A Pareto chart is a bar chart where bars are ordered in decreasing magnitude. The greater the bar magnitude, the more effect its corresponding factor (or interaction) has on the response. In the Pareto chart the following symbol set is used: polymer-melt temperature (A), mould temperature (B), holding pressure (C), injection speed (D) and cooling time (E).

In figure 4a main effect are plotted for each of the input parameters, with mass as the output parameter. Hence, for example, the first graph of figure 4a is a plot of mass against melt temperature (A).

In figure 4b factor effects are plotted as a bar chart, which are related to the averages of the main-effect plots. Briefly, if Δ is the difference between the two averages of the response points for a particular factor, i.e. the difference between the two points connected by the sloped line, then the effect bar corresponding to that particular factor is the absolute value of half the effect, i.e. |Δ/2| (Lahey and Launsby 1998).

Figure 4b plots both the main input parameters, for example, C the holding pressure, and the interactions between input parameters, for example, BE, the interaction between the mould temperature and the cooling time. The vertical line on the figure corresponds to the threshold beyond which factors become statistically significant at the significance level determined by the value of alpha. This value is determined from the t-distribution, where t is the 1-(alpha/2) quantile of the distribution (Minitab Inc. 2009). The significance of the effect can be found by the relationship of the histogram value to this line. The alpha value, also referred to as the level of significance, is a measurement of risk in detecting effects, and is expressed as a probability between 0 and 1. An alpha value of 0.05 indicates that the chance of finding an effect that does not exist is only 5% (a confidence limit of 95%).

Figures 5 to 8, representing the screening experiment data for parts *b* to *e*, are plotted using the same approach.

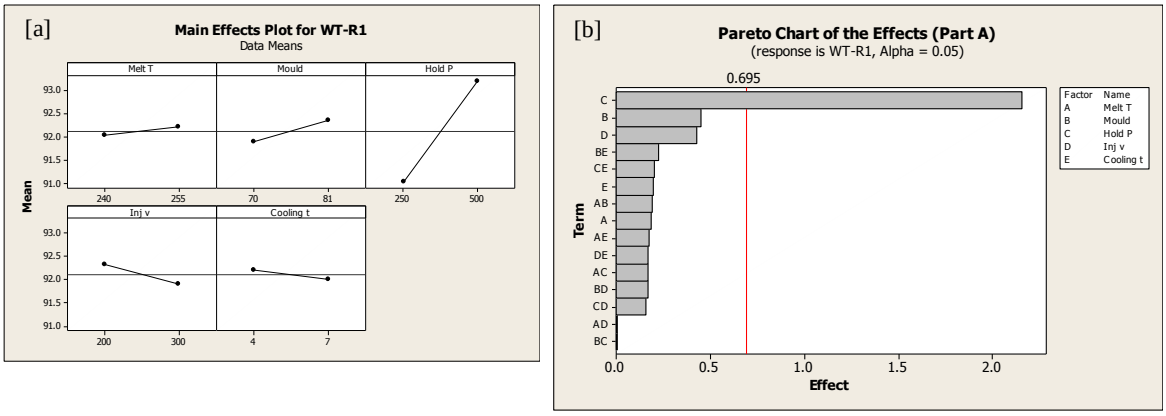

Fig 4 Screening results for part *a*: [a] Main effects plot, and [b] Pareto chart

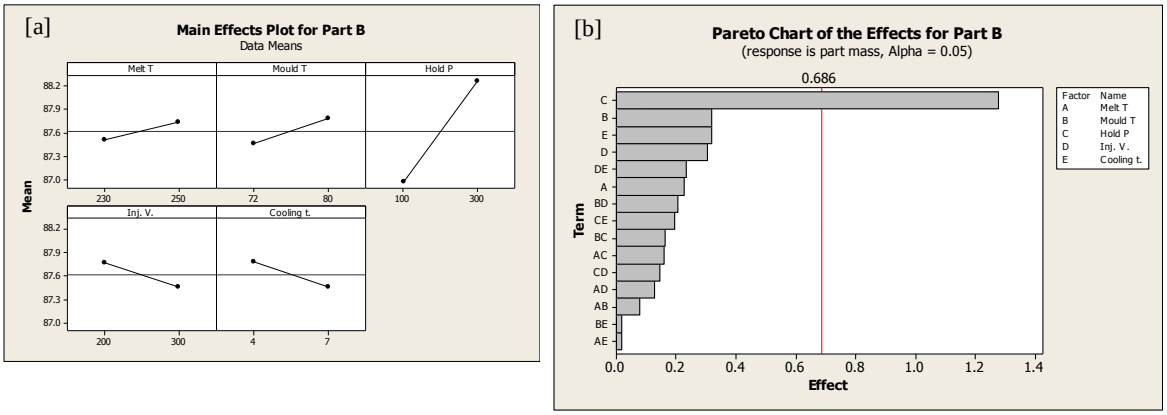

Fig 5 Screening results for part *b*: [a] Main effects plot, and [b] Pareto chart

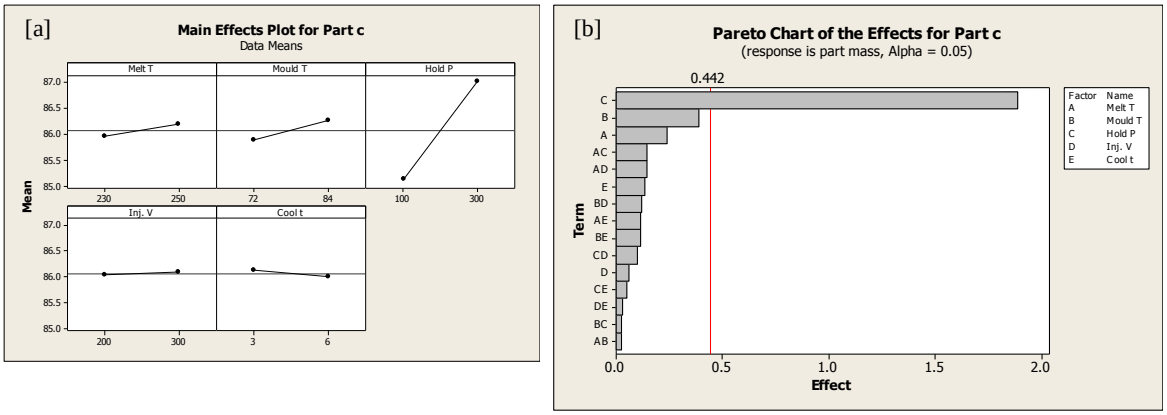

Fig 6 Screening results for part *c*: [a] Main effects plot, and [b] Pareto chart

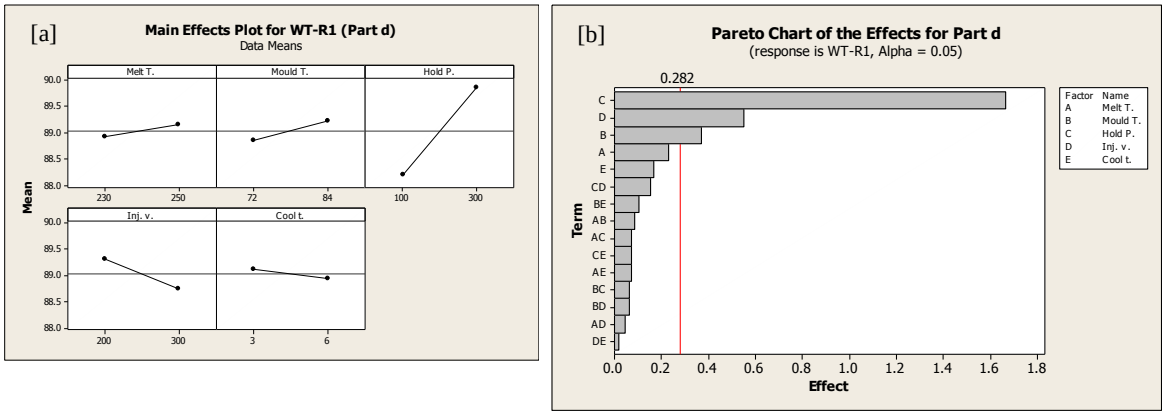

Fig 7 Screening results for part *d*: [a] Main effects plot, and [b] Pareto chart

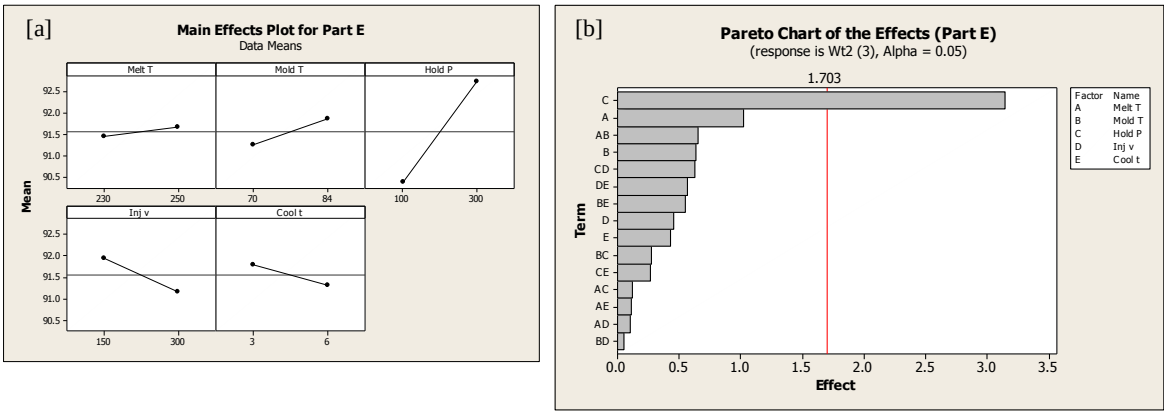

Fig 8 Screening results for part *e*: [a] Main effects plot, and [b] Pareto chart

3.2. Desirability function processing conditions

Table 5 tabulates desired part mass, the calculated optimum values of the process parameters to achieve these mass values and actual part mass obtained experimentally at these processing conditions.

The desired part masses were derived from the screening experiments. The moulded samples are inspected, and the completely filled samples are identified and weighed. The average mass of the complete samples is used as the "target" mass for the desirability function. The minimum and maximum masses of the completely filled samples are input as the lower and upper limits for the target mass, respectively. They are tabulated in table 5 as the target mass and a minimum and maximum acceptable mass value.

The experimental conditions, i.e. the levels of the input parameters, predicted to achieve those masses are outputs of the desirability function. These are tabulated in table 5 for each of the five input variables (denoted as "required levels").

In table 5, the "experimental mass" is the average mass of ten samples collected randomly after the moulding machine had reached stability. The minimum and maximum values are the mass of the samples with lowest and highest mass magnitude within the ten samples, respectively.

Part	Desired mass [mg]			Required levels of process parameters					Experimental mass [mg]		
	Target	Min.	Max.	T_p [°C]	T_m [°C]	V_i [mm/s]	P_h [bar]	t_c [sec]	Avg.	Min.	Max.
a	93.1	92.6	93.6	250	81	200	416	4	93.1	92.9	93.3
b	88.6	88.2	89.0	250	80	200	300	4	88.7	88.4	88.9
c	86.5	86.0	87.0	250	81	300	170	3	86.7	86.2	86.9
d	90.0	89.6	90.4	250	84	200	300	3	90.1	89.9	90.3
e	92.5	92.0	93.0	243	84	300	300	3	92.0	91.8	92.2

Table 5. Required masses and limits, calculated optimum parameters and corresponding experimental results.

4. Discussion

4.1. Screening stage

Figures 4 to 8 show a significant effect of holding pressure for all the five parts, with four parts, *a*, *b*, *c* and *e*, showing it as the only significant effect. This substantial effect was also visible during the experiments, as all samples that were produced at a lower level of holding pressure exhibited evidence of incomplete filling, regardless of the levels of the other four parameters. In contrast, cooling time had no effect for any of the parts.

For Part *d*, three significant effects were observed: holding pressure, injection velocity and mould temperature. However, aside from Part *d*, mould temperature and injection velocity had no apparent effect on the mass of other parts.

The importance of holding pressure lies in the fact that it overcomes the tendency of the polymer melt to prematurely freeze before the injection process is complete. Premature freezing is likely to be exacerbated by the relatively high rate of heat transfer between the polymer and the mould walls for parts with micro-scaled dimensions. In prior work (Zhao et al. 2003a; Zhao et al. 2003b), metering volume and holding pressure time were used as factors. In this work, metering size was kept constant, as it was determined from the familiarization stage (Section 2.4.1), and the holding pressure value was used rather than the holding pressure time. It is possible that both the holding pressure magnitude and time (or their interaction) would be significant if they are used together as factors in a more extended DOE plan.

The lack of significance of cooling time is consistent with previous work (Zhao et al. 2003a; Zhao et al. 2003b). This is because the effect of cooling in injection moulding is usually associated with changes in the component geometry (e.g. shrinkage, warpage) (Osswald 2001), but the cooling scheme does not have the same effect on the part weight as its effect takes place after the cavity is already filled.

The lack of significance of mould temperature may lie in the selection of the two levels at values below the T_g of the polymer. This is consistent with the data presented in (Shen et al. 2002) where increasing the mould temperature improved the filling quality, although all the experiments were performed while the mould temperature was below the Tg of the PMMA. It is less consistent with the numerical simulation data of (Zhao et al. 2003a) which predicted short shots unless the mould temperature was raised above the Tg of the PMMA.

The general tendency found here of the lack of significance of melt temperature was also found in prior work. For small part volumes, like those found in micro-moulding, the melt temperature decreases at a very high rate once the polymer contacts the cavity walls, as long as the mould temperature is kept below the melt temperature of the polymer (Yao and Kim 2004). In the work presented here, both the high and low levels of the mould temperature were kept below Tg. Hence, by the time the polymer filled the part cavity it would have seen a significant reduction in its temperature.

The lack of significance of the injection velocity as a parameter may lie in the relatively small change of shear rate associated with changing between the two levels of injection velocity. The relation between shear rate and injection velocity can be approximated by (Osswald 2001):

$$\dot{\gamma} = \frac{4\dot{Q}}{\pi r^3} \qquad (4)$$

where $\dot{Q}$ is the volume flow rate, and r is the radius of the flow path cross section (in this case the part gate). The flow rate is a function of the injection speed V_i, so equation (4) can be rewritten as:

$$\dot{\gamma} = \frac{4V_i R^2}{r^3} \qquad (5)$$

where R is the radius of the injection plunger.

Since the gates have a rectangular cross section (1 x 0.5 mm), the equivalent hydraulic diameter may be used in equation (5) to estimate the value of r. The calculated shear rates based on low-level and high-level value for injection velocity both have an order of magnitude of 10^5 s^{-1}. Shear rate vs. viscosity data for the PMMA grade used indicates that these shear rates correspond to viscosities in the order of 10^1 Pa.s at 230°C at which no significant shear-thinning behaviour would be observed.

4.2. Desirability function processing conditions

Table 5 presented the suggested processing parameters for improved filling, which are obtained by meeting the conditions listed in equation (3). It should be noted that the desirability function cannot recommend parameter values outside the lower and high levels of the factors. Whilst certain parameter values in table 5 lie between the high and low levels, the majority lie either at the high level or the low level. This is indicates that the desirability function might have recommended an even higher or lower level of the parameter, had the original levels been more widely spread.

Table 5 shows also that the average masses of the parts produced under the conditions predicted by the desirability function lie within 0.5% of the specified target values. All the produced parts were within the mass upper limit pre-set in the function, but for Parts *b* and *e*, some of the produced samples were under the lower limit by approximately 0.2 mg.

Figure 9 shows an example of how the desirability function improved the filling quality of the parts. Figure 9 (a) shows a view of a sample of Part *d* from the screening stage (run 5) where some areas of the edges that are close to the last filled point are incomplete. Voids can also be seen on the surface around the cylindrical hole. Figure 9 (b) shows the same part after application of the desirability function, where the edges are completely filled and voids are no longer apparent on the part surface.

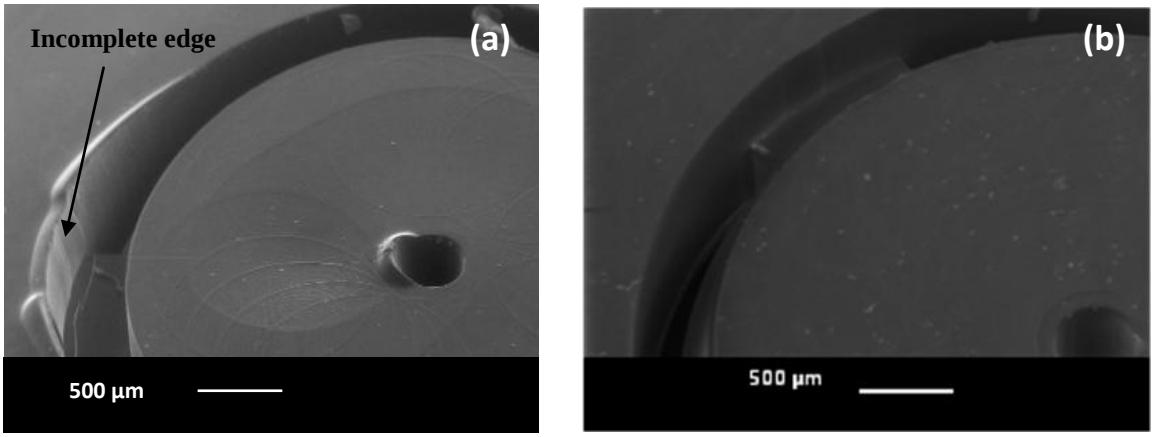

Fig 9 SEM micrograph of samples of Part *d*. 4(a) an example before applying the desirability function (T_p = 230°C, T_m =72°C, V_i = 300 mm/s, P_h = 100 bar and t_c = 3 s); 4(b) after applying the desirability function (T_p = 250°C, T_m =84°C, V_i = 200 mm/s, P_h = 300 bar and t_c = 3)

Table 5 shows the data from applying the desirability function independently to each part. However, an individual-part desirability function approach is difficult to extend to a prediction of any compromise parameters which would be result in relatively high filling quality for all the five parts if they were produced by a single mould in one shot.

One method to achieve such a compromise might be to discern if there were general trends that could be observed when comparing the desirability function to the screening parameters, and then apply these trends in required process parameters to establish compromise conditions. In effect, this means comparing the required levels of process parameters in table 5 with the envelope of parameter high and low levels of table 2. Such a comparison does show that general trends are present, independent of the part shape. The desirability function predicts that setting the melt temperature, mould temperature and holding pressure to their high levels would generally result in better filling, as does, with a few exceptions, setting the injection velocity and cooling temperature to their low levels.

Table 6 shows a set of compromise processing conditions constructed following these general trends in desirable process parameters. To test this prediction, the micro-mould was reconfigured such that all the five parts are injected through a common runner system, and parts processed using the conditions of table 6:

Parameter	**T_p [°C]**	**T_m [°C]**	**V_i [mm/s]**	**P_h [bar]**	**t_c [s]**
Value	250	84	200	300	3

Table 6. Processing parameters for a five-part micro-moulded component.

The produced part is shown in figure 10, where all the parts were checked under the microscope to be completely filled.

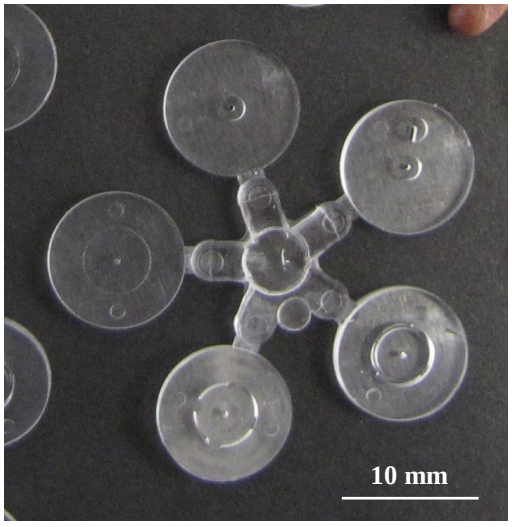

Fig 10 A photograph of a completely filled, five-part plastic component produced under compromise conditions

4.3. Effect of part geometry

The results shown in figures 4 to 8 provide some information on the effect of the mould geometry on the filling quality of the part.

As noted in section 4.1, for Part *d*, other effects, in addition to the holding pressure, were of significance in filling quality. It seems likely that this is owing to the relatively high geometrical complexity of this part in comparison to the other parts. This complexity is generated from the

four micro-scaled flow paths that exist in Part *d*, which represent a rapid change in part thickness that imposes 'extra resistance' on the flow of the material to completely fill the cavity. Figure 11 presents photographs of mouldings of Parts *a* and *d*, as being at the two extremes of geometrical complexity amongst the five moulded parts. The mouldings are 'short shots' produced to visualise the difference in filling sequence between the two parts.

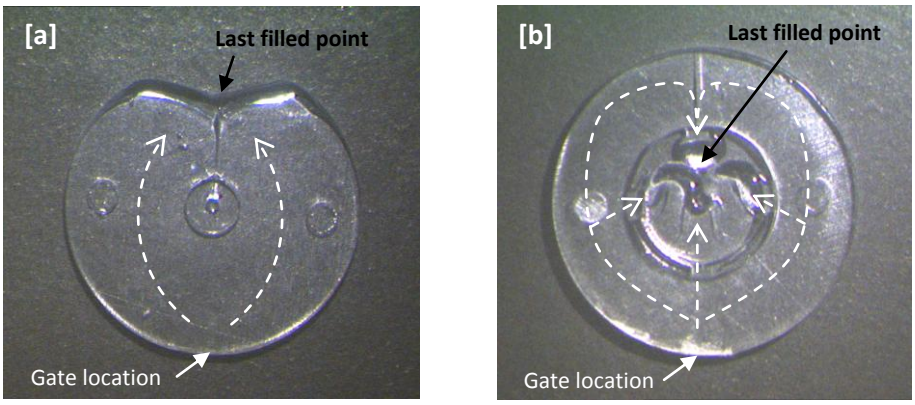

Fig 11 (a) Short shot of Part *a*. (b) Short shot of Part *d*

In Part *a* the last filled point is located at the far end of the flow path, whereas in Part *d* the last filled point is located close to the centre. Such differences are expected as a consequence of the 'hesitation effect' commonly seen in polymer flow, where, in cavities with varying thickness values, polymer melts tend to fill areas with larger thickness before they flow into smaller thicknesses. In Part *a*, where the part thickness is uniform, the polymer fills the cavity gradually as the flow path is divided at the central "pin" of the mould and then rejoins afterwards forming a weld line. In Part *d*, the rapid change in thickness causes the polymer flow to experience hesitation during the filling process, and a higher injection pressure will be required for the polymer to flow through these features. Larger flow-path cross-sections, for example the perimeter of the shape in Part *d*, are filled before the polymer starts to pass through the four "openings" at the centre area of the part (see figure 1 Part *d*).

Owing to the relatively small dimensions of each of the four openings (500 x 600 μm) a high possibility of premature freezing would be expected at these locations. Similarly to conventional injection moulding, the cooling time of the polymer during micromoulding is dependent, among other factors, on the part thickness squared (Yao and Kim 2004). This indicates that the cooling process in Part *d*, where, in the four opening areas, the minimum thickness is 500 μm, is much faster than, for example, Parts *a* and *b*, where the minimum thickness is 950 μm to 1 mm.

The rapid decrease in thickness does not only affect the freezing process, but it also influences other parameters. As suggested in the literature (Yao and Kim 2004), as the part thickness decreases to fractions of a millimetre, a drastic increase is observed in the injection pressure required to fill the cavity, and a higher possibility of incomplete filling is expected. This is particularly observed for cold-mould filling, i.e. when mould temperature is lower than the melt temperature, as is the case in this work. This explains why mould temperature becomes significant at such rapid changes in thickness as seen in Part *d*. Part thickness also affects the role of injection speed on the required filling pressure. As the thickness decreases, the variation in injection speed becomes more significant in affecting the injection pressure required to fill the mould cavity (Yao and Kim 2004).

5. Conclusions

In order to investigate the effect of part geometry on moulding parameters, this paper investigated the moulding parameters of five different micro-parts using mass as an experiment response. Parts differed in the through-hole and surface geometries, but had a constant outer radius and similar thicknesses. The same polymer, a PMMA grade, was used throughout the experiments.

A three-stage design of experiments approach consisting of feasibility, screening and desirability function, was undertaken to evaluate the filling quality in micro-injection moulding and correlate it to the processing parameters. It was shown that holding pressure was the main influential processing parameter for all of the part geometries.

A comparison of desirable moulding parameters for different part geometries, showed the influence of geometry on processing conditions. Sharp changes in thickness within a part correlated with an increase in the number of significant moulding parameters. For a complex part, injection speed and mould temperature became statistically significant.

For each part, a desirability function was used to specify a combination of processing conditions that would improve filling quality. The produced parts had average masses that were within 0.5% of the target values.

Comparing the desirability function predictions with the high and low parameter values of the screening stage showed, with some exceptions, that regardless of part geometry, desirability function predictions for a particular process parameter exhibited clustering behaviour. These trends in clustering behaviour were used to produce a set of compromise moulding conditions to micromould a multi-part component. Multi-part components moulded using these parameters exhibited complete filling in each of the five parts.

References

Attia UM, Marson S and Alcock JR (2009) Micro-injection moulding of polymer microfluidic devices. Microfluid Nanofluid 7:1-28

Aufiero R (2005) The effect of process conditions on part quality in microinjection molding. ANTEC: Proc Annual Technical Conf (Boston, MA, 1-5 May 2005):36-40

De Mello A (2002) Plastic fantastic? Lab Chip 2:31N-36N

Eriksson L, Johansson N, Kettaneh-Wold N, Wikstrom C and Wold S (2008) Design of experiments: principles and applications, 3rd edn. Umetrics, Umeå

Griffiths CA, Dimov S, Brousseau EB, Chouquet C, Gavillet J and Bigot S (2008) Micro-injection moulding: surface treatment effects on part demoulding. Proc 4M2008 (Cardiff, UK, 9th - 11th September 2008)

Griffiths C, Dimov S, Brousseau EB and Hoyle RT (2007) The effects of tool surface quality in micro-injection moulding. J Mater Process Tech 189:418-27

Jung W-C, Heo Y-M, Shin K-H, Yoon G-S and Chang S-H (2007) An experimatal study on micro injection paramaters. ANTEC: Proc Annual Technical Conf (Cincinnati, OH, 6-11 May 2007): 638-642

Lahey JP and Launsby RG (1998) Experimental design for injection molding. Launsby Consulting, Colorado Springs, CO

Lee B-K, Hwang CJ, Kim DS and Kwon TH (2008) Replication quality of flow-through microfilters in microfluidic lab-on-a-chip for blood typing by microinjection molding. J Manuf Sci E-T ASME 130:0210101-0210108

Marson S, Attia UM, Allen DM, Tipler P, Jin T, Hedge J and Alcock JR (2009) Reconfigurable micro-mould for the manufacture of truly 3D polymer microfluidic devices. Proc CIRP Design Conf (Cranfield, UK, 30-31 March 2009):343-346

Minitab Inc. Available at: www.minitab.com. Accessed 2009

Mönkkönen K, Hietala J, Pääkkönen P, Pääkkönen EJ, Kaikuranta T, Pakkanen TT and Jääskeläinen T (2002) Replication of sub-micron features using amorphous thermoplastics. Polym Eng Sci 42: 1600-1608

Montgomery DC (2005). Design and analysis of experiments, 6th edn. Wiley, Hoboken, Great Britain

Osswald T, Turng L and Gramann P (Editors) (2001) Injection molding handbook. Hanser/Gardner Publications, Cincinnti, OH

Pirskanen J, Immonen J, Kalima V, Pietarinen J, Siitonen S, Kuittinen M, Mönkkönen K, Pakkanen T, Suvanto M and Pääkkönen EJ (2005) Replication of sub-micrometre features using microsystems technology. Plast Rubber Compos 34:222-226

Sha B, Dimov S, Griffiths C and Packianather MS (2007a) Investigation of micro-injection moulding: factors affecting the replication quality. J Mater Process Technol 183:284-296

Sha B, Dimov S, Griffiths C and Packianather MS (2007b) Micro-injection moulding: factors affecting the achievable aspect ratios. Int J Adv Manuf Technol 33:147-156

Shen YK, Yeh SL and Chen SH (2002) Three-dimensional non-Newtonian computations of micro-injection molding with the finite element method. Int Commun Heat Mass 29:643-652

Tosello G, Gava A, Hansen HN and Lucchetta G (2007) Influence of process parameters on the weld lines of a micro injection molded component. ANTEC: Proc Annual Technical Conf (Cincinnati, OH, 6-11 May 2007):2002-2006

Wimberger-Friedl R (2000) Injection molding of sub-µm grating optical elements. J Inject Molding Technol 4:78-83

Yao D and Kim B (2004) Scaling issues in miniaturization of injection molded parts", J Manuf Sci Eng Trans ASME, vol. 126, no. 4, pp. 733-739.

Yao D and Kim B (2002) Injection molding high aspect ratio microfeatures. J Manuf Sci E-T ASME 126:11-17

Zhao J, Mayes R, Chen G, Xie H and Chan P (2003a) Effects of process parameters on the micro molding process. Polym Eng Sci 43:1542-1554

Zhao J, Mayes R, Chen G, Chan PS and Xiong ZJ (2003b) Polymer micromould design and micromoulding process. Plast Rubber Compos 32:240-247